

RESEARCH

Open Access



Biosynthesized silver nanoparticles and miR34a mimics mediated activation of death receptor in MCF-7 human breast cancer cell lines

Muhammad Javed Iqbal^{1,2}, Umer Rashid^{1*}, Zeeshan Javed^{3*}, Zara Hamid¹, Komal Imran², Ayesha Kabeer², Shahid Raza³, Zainab M. Almarhoon⁴, Željko Reiner⁵, Iulia-Cristina Bagiu^{6,7}, Radu Vasile Bagiu⁸, Ioan Sarac⁹, Javad Sharifi-Rad^{10*}, Alibek Ydyrys¹¹, Sevgi Durna Daştan^{12,13}, Monica Butnariu^{9*} and William C. Cho^{14*}

*Correspondence:
umer.rashid@uog.edu.pk;
zeeshan_javed456@yahoo.com;
javad.sharifirad@gmail.com;
monicabutnariu@yahoo.com;
chocs@ha.org.hk

¹ Department of Biochemistry and Biotechnology, University of Gujrat, Gujrat, Pakistan

³ Office of Research Innovation and Commercialization, Lahore Garrison University, Lahore, Pakistan

⁹ University of Life Sciences "King Mihai I" from Timisoara, 300645, Calea Aradului 119, Timis, Romania

¹⁰ Facultad de Medicina, Universidad del Azuay, Cuenca, Ecuador

¹⁴ Department of Clinical Oncology, Queen Elizabeth Hospital, Kowloon, Hong Kong
Full list of author information is available at the end of the article

Abstract

Nano-biotechnology-based clinical applications to cure health-related issues have gained huge attention among the scientific community and hold great promise to limit cancer metastasis. In this study, green-derived silver nanoparticles were synthesized by using leaf extract of *Litchi chinensis*. Characterization of biosynthesized silver nanoparticles was performed by using UV–Vis spectroscopy, FTIR, XRD, EDS, and SEM analysis. The clinical application of green-drive nanoparticles was investigated by using MCF-7 cancer cell lines. MCF-7 breast cancer cell lines were analyzed against three different treatments. (i) Silver nanoparticles (AgNPs), (ii) miR34a mimics and (iii) Co-delivery of AgNPs and miR34a mimics. Cell viability was determined by MTT assay and, extraction of mRNA and cDNA synthesis were performed after successful cellular transfection. qRT-PCR was done for expression analysis of DR4 and DR5 upon exogenous delivery of all 3 treatments. Results indicate that *L. chinensis* leaves have a significant amount of phenolic and flavonoid contents and also possess massive antioxidant activity. The diameter of nanoparticles was observed in the range of 41–55 nm. It was concluded that green-derived silver nanoparticles can be a potential contributing agent for cancer prevention and are reported to upregulate the expression of DR4 and DR5 by 0.8-folds and 3.7-folds, respectively.

Keywords: MCF-7 cell lines, Silver nanoparticles synthesis, DR4, DR5, Breast cancer

Introduction

Breast cancer is the most commonly occurring cancer in women and is reported to be the second leading cause of cancer death among women. Globally, it is the fifth most common cancer associated with mortality (Han et al. 2017a). Pakistan, being the sixth largest populated country, stands at the crossroad in the battle against cancer. Complex cellular mechanisms of cancer cells make it more difficult to understand the molecular puzzle of the disease. Apoptosis is a natural cell death process that the biological system



© The Author(s) 2022. **Open Access** This article is licensed under a Creative Commons Attribution 4.0 International License, which permits use, sharing, adaptation, distribution and reproduction in any medium or format, as long as you give appropriate credit to the original author(s) and the source, provide a link to the Creative Commons licence, and indicate if changes were made. The images or other third party material in this article are included in the article's Creative Commons licence, unless indicated otherwise in a credit line to the material. If material is not included in the article's Creative Commons licence and your intended use is not permitted by statutory regulation or exceeds the permitted use, you will need to obtain permission directly from the copyright holder. To view a copy of this licence, visit <http://creativecommons.org/licenses/by/4.0/>. The Creative Commons Public Domain Dedication waiver (<http://creativecommons.org/publicdomain/zero/1.0/>) applies to the data made available in this article, unless otherwise stated in a credit line to the data.

uses as a filter to destroy abnormal cells. This controlled cell death process is dependent upon the upregulation of death receptor 4 (DR4) and death receptor 5 (DR5) involving Bcl-2, CASP8, CASP10, Bik, Bak, and many other key signaling molecules (Gaur and Aggarwal 2003; Kiraz et al. 2016).

Green leaves of herbal plants are reported to be used from ancient times for medicinal purposes. Phenols are the key components of plants possessing scavenging ability and anti-proliferative effect because of their structural hydroxyl group. Phenols stimulate antioxidant activity by neutralizing highly reactive free radicals, and reactive oxygen species, such as peroxide and superoxide, in cells and thereby, reducing oxidative damage and oxidative stress. It is observed that total phenolic contents and total flavonoid contents of the selected medical plant leaves have a significant anti-proliferative effect (Carvalho et al. 2010; Fu et al. 2011). The flavonoids, phenols, and condensed tannins found in litchi leaves have significant antioxidative and anti-inflammatory properties. It is also reported to have anti-cancer, diuretic, hypoglycemic, anti-bacterial, anti-platelet, anti-hyperlipidemic, and antiviral properties. Olive leaf extract is used as a reducing and capping agent for the synthesis of silver nanoparticles. It contains antiviral, antioxidant, antimicrobial, anticancer, anti-inflammatory, and hypoglycemic properties. Green tea leaves are believed to have optimal phenolic content and high antioxidant activity, because they are rich in bioactive phytochemicals that are used as anti-septic, anticancer, and antibacterial agents for valuable medical treatments.

Silver nanoparticle synthesis is reported to be carried out by different methodologies and it has been shown that the green approach is more efficacious in limiting and inhibiting microbial growth and cancer progression, respectively (Ahmed et al. 2016; Iqbal et al. 2018). The characterization of nanoparticles is an essential step for further analysis of nanoparticles. Characterization helps to determine the potential size, shape, composition, purity, concentration, functional groups, crystalline nature, and morphology (Pathak and Thassu 2016). Biosynthesized silver nanoparticles, and microRNA-34a (miR-34a) mimics are also believed to inhibit cancer progression by transcriptionally modulating the pathways involving p53, Bcl2, and transforming growth factor β (TGF- β) signaling molecules, and epithelial–mesenchymal transition (EMT) (Imani et al. 2017).

Non-coding (nc) RNAs are recognized to play a vital role in human growth and normal development. Among this broad family of ncRNAs, microRNAs have been associated with the onset of various diseases including cancer. MicroRNA miR34a is clinically proven as a master regulator of tumor suppression. Clinical trials of miR34a are under investigation to understand the complex molecular networking of cancer progression in the human biological system. miR34a is reported to suppress various regulators of cancer cell proliferation. It is believed that the expression of miR34a is regulated by the guardian of the human genome “p53”. P53-dependent tumor suppression mechanism is believed to trigger a protective response in the cell. It is observed that miR34a expression is downregulated in many cancers and has the potential to affect over 700 downstream transcripts and p53 regulation as well. The objective of this study is exogenous delivery of miR34a mimics to restore p53 functionality and induce apoptosis in cancerous cells as potential replacement therapy. In addition, silver nanoparticles synthesized by the green approach (*Litchi chinensis*) can also be used as an independent and combined therapy against cancerous cell lines.

Materials and methods

Sample collection

Litchi chinensis leaves were collected from the lychee garden in Sharaqpur, Lahore. Olive leaves and green tea leaves were collected from Barani Agriculture Research Institute (BARI) Chakwal and Abbottabad tea gardens, respectively. Silver nitrate, DPPH, Superscript first-strand system kit (Invitrogen), and bacterial strains were available at the Biotechnology laboratory, university of Gujrat. Cancerous cell lines, MTT assay and RT-PCR facility were available at collaborative institute IBGE, KRL hospital Islamabad. MISSION[®] microRNA Mimics “hsa-miR-34a” were purchased from Sigma Aldrich. Opti-MEM[™] Reduced serum medium and lipofectamine 3000 transfection reagent were purchased from Thermo Fisher Scientific.

Preparation of leaves extract

Leaves of *Litchi chinensis*, green tea, and olives were selected as source materials for the synthesis of silver nanoparticles. To determine the biological activity and efficacy of leaf extracts, extracts were prepared by using three different solvents, including water, chloroform, and ethanol. 15 g of fine powder of each green source was dissolved in 300 ml of each solvent and subjected to a shaking water bath incubator at 37 °C for 48 h. Each solvent was then filtered through Whatman paper no. 1 by using vacuum filtration and further processed to make it more concentrated by using a rotary evaporator. Each of the concentrated extracts was transferred to 15 ml falcon tubes separately for further biological evaluation or stored at 4 °C (He et al. 2002).

Leaf extracts from all three sources were used to determine their total phenolic content, total flavonoid content, and antioxidant activity.

Total phenolic content (TPC)

Total phenolic contents of the three green source extracts (*Litchi chinensis*, green tea, and olive leaves) were determined by using the spectrophotometric method. The reaction mixture was prepared by mixing a 20 µl solution of leaf extract (50 mg/ml DMSO) of different concentrations in Eppendorf tubes. 490 µl of 50% Folin–Ciocalteu’s reagent (FCR) was added into Eppendorf tubes. 490 µl of 6% sodium carbonate solution was added to the test tubes. 6% NaHCO₃ and distilled water were added to make the total volume up to 1000 µl in an Eppendorf tube. The absorbance was determined by using a spectrophotometer at 725 nm/760 nm against blank (Abdelhady and Badr 2016).

Total flavonoid content (TFC)

Total flavonoid contents were determined by aluminum chloride colorimetric methodology. 20 µl of each plant extract was taken into separate Eppendorf tubes. 60 µl of methanol was added to it. 100 µl of 10% AlCl₃ solution was added to each Eppendorf tube. 100 µl of 1 M potassium acetate (KCH₃CO₂) solution was also added to it. 720 µl of distilled water was added to make the total volume of the mixture up to 1000 µl in

each Eppendorf tube. The samples were incubated for 30 min at 37 °C in the incubator. Afterward, the absorbance was determined using a spectrophotometer at 420 nm.

Determination of antioxidant activity

The antioxidant and free radical scavenging activity of all extracts were determined by DPPH free radical scavenging method through the spectrophotometer. 15 µl of each of the plant extracts was added into a separate Eppendorf tube and freshly prepared 300 µM DPPH solution (1.5 ml) was then added into each Eppendorf tube to get a final concentration of 1000 µg/ml, 750 µg/ml, and 500 µg/ml. After incubation in darkness at 37 °C for 30 min, the change in color (from deep purple to yellow) was determined at the absorbance of 515 nm using a UV–Vis spectrophotometer. DMSO and ascorbic acid were used as negative and positive controls. Each experiment was performed in triplicate (Abdelhady and Badr 2016).

Green synthesis of silver nanoparticles

Litchi chinensis extract was observed to be an ideal candidate among other green sources based upon TPC and TFC analysis and was selected as the green source for the onward synthesis of silver nanoparticles. 2.5 ml of leaf extract of *Litchi chinensis* was mixed in 50 ml of 1 mM aqueous silver nitrate solution. The filtered plant extract was added dropwise and a bio-reduction reaction was performed at room temperature (Chatterjee et al. 2015). Each sample was incubated for 1–2 h and the pH was adjusted to 8 using a pH meter.

Characterization of biosynthesized silver nanoparticles

The absorption spectrum of leaf extracts, aqueous 1 mM silver nitrate solution and the solution for biosynthesized silver nanoparticles was obtained by using a JASCO UV–Vis 530 spectrophotometer within the range of 200–800 nm (Awwad and Salem 2012). Functional groups responsible for capping and stabilization of nanoparticles were detected by Fourier transform infrared analysis (FTIR). Freeze-dried powder of leaves extract, and silver nanoparticles were placed on a fresh glass slide and analyzed for the FTIR analysis (Awwad and Salem 2012). The crystalline nature of the biosynthesized silver nanoparticles was determined by an X-ray diffractometer (XRD). XRD operated at 40 kV and 30 mA, while the patterns were recorded using a Cu anode having a $K\alpha$ radiation wavelength of about 1.54060 Å (Khalil et al. 2014). Metallic silver presence was detected using energy dispersive spectroscopic (EDS) analysis. The morphology and size distribution of silver nanoparticles was determined by scanning electron microscopy (SEM).

Cellular transfection of MCF-7 breast cancer cell line

Human breast adenocarcinoma cell line “MCF-7” (Michigan Cancer Foundation-7) was used and cytotoxic activity was investigated by MTT assay (Han et al. 2017b). Transfection of miR34a and silver nanoparticles into cancerous cells was achieved by using Lipofectamine 3000 transfection reagent and their expression analysis was investigated using quantitative RT-PCR.

MicroRNA (miR34a) mimics are the synthetic version of biomolecules and were purchased from Sigma Aldrich (MISSION microRNA Mimics). miR34a mimics were also used in combination with silver nanoparticles to evaluate the co-transfection effect on cancer cell lines and to analyze the gene expression of targeted genes exposed to different treatments. Cells were cultured in 96 well plates to achieve 70–90% confluency ($1-4 \times 10^4$ cells) at the time of transfection. For effective cellular intake of desired microRNA and silver nanoparticles, the optimal result was obtained by using an Opti-MEM reduced serum medium.

RNA extraction

After successful MCF-7 cell culturing and growth, transfection of miR34a and silver nanoparticles was carried out by using lipofectamine 3000 reagent. RNA was extracted from 10^6 cells, and media was aspirated and washed once with ice-cold PBS. Dead cells were removed if any, and 1 ml of trizol was added. Cells were scrubbed briefly and trizol was removed. Trizol cell lysate was shifted into a 1.5 ml Eppendorf tube. Afterward, 250 μ l chloroform was added and shaken vigorously for 15 min. Eppendorf tube was incubated for 5 min at room temperature. Centrifugation was performed at 10,000 rpm for 5 min. The aqueous layer was removed and shifted into a new Eppendorf tube. 550 μ l of isopropanol was then added to the aqueous layer and mixed gently. The tube was then incubated for 5 min at room temperature and centrifuged at 14,000 rpm for 30 min. Samples were placed on ice and the supernatant was discarded. 75% ethanol was added to the sample and centrifuged at 9500 rpm for 6 min. The supernatant was discarded. Pellet was air-dried and 20 μ l of diethylpyrocarbonate (DEPC) treated water was added to it.

cDNA synthesis

After successful RNA extraction and purification, RNA quantification was performed by nanodrop spectrophotometer and was 1000 ng. Superscript first-strand system kit (Invitrogen) was used for cDNA synthesis. Oligo DT primers, 10 mM dNTPs, DEPC water, 5 \times RT buffer, and RNase inhibition were used and centrifuged in PCR tubes. After incubation at 38 °C for 3 min, 1 μ l reverse transcriptase was added and incubated at 38 °C for 50 min to synthesize cDNA. Afterward, the sample was subjected to heating for 15 min at 70 °C according to the manufacturer's protocol and then stored at – 20 °C.

qPCR expression analysis

mRNA expression upon the delivery of silver nanoparticles, miR34a mimic, and co-delivery of miR34a and silver nanoparticles in cell lines was quantified through qPCR. Expression analysis was performed by taking the GAPDH gene as the housekeeping

Table 1 Primers for genes of interest and housekeeping genes

Genes	Forward primer	Reverse primer
DR4	5'-TCCAGCAAATGGTGCTGAC-3'	5'-GAGTCAAAGGGCACGATGTT-3'
DR5	5'-CCAGCAAATGAAGGTGATCC-3'	5'-GCACCAAGTCTGCAAAGTCA-3'
GAPDH	5'-TGCACCACTGCTTAG-3'	5'-GGATGCAGGGATGATGTT-3'

gene, DR4, and DR5 as target genes (Table 1). Ct value was noted. An average Ct value was calculated by the use of the $\Delta\Delta C_t$ and Livak method, while fold difference was obtained to measure the expression level of both targeted genes by taking GAPDH as an internal control (Livak and Schmittgen 2001). qRT-PCR was performed using SYBR Green mini kit according to the manufacturer's protocol.

Bioinformatic tool to establish signaling pathway

Bioinformatic tool "Genemania" was used to establish molecular signaling pathways of targeted genes including DR4, and DR5 that have an important role in the progression of multiple human diseases, including cancer.

Results

Total phenolic content (TPC)

The total phenolic content of three different leaf extracts was measured by taking three different solvents. For *Litchi chinensis* leaf extracts, 17.7 ± 0.2 mg/g, 17.2 ± 0.2 mg/g, and 16.5 ± 0.2 mg/g were observed for aqueous, chloroform, and ethanol solvent, respectively. For green tea leaf extracts, 15.5 ± 0.2 mg/g, 14.9 ± 0.2 mg/g, and 13.2 ± 0.2 mg/g were noted by using aqueous, chloroform, and ethanol solvents, respectively. Olive leaves extracts had the lowest TPC average of all three solvents (Fig. 1).

Total flavonoid content (TFC)

Total flavonoid content measured in aqueous, chloroform, and ethanol extracts of *Litchi chinensis* was 170.0 ± 0.01 mg/g, 166.0 ± 0.5 mg/g, and 161.0 ± 0.1 mg/g, respectively. However, the flavonoid content in green tea ethanol extract was higher 165.0 ± 0.06 mg/g than the other two solvents. In the case of olive extracts, the chloroform extract had the lowest flavonoid content 158.0 ± 0.1 mg/g (Fig. 2).

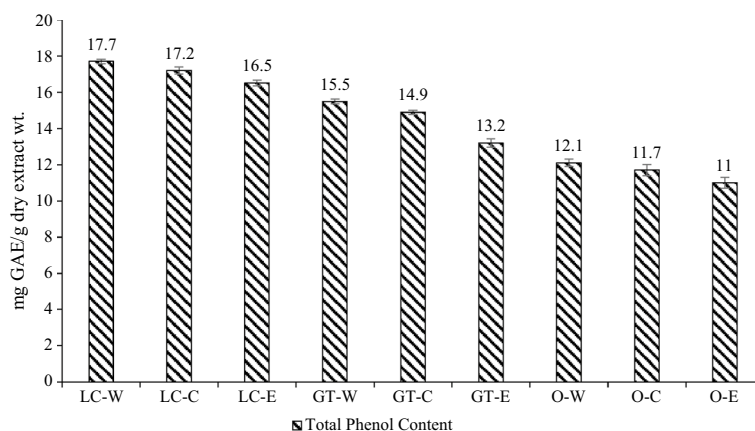


Fig. 1 Total phenolic content (TPC) of leaf extracts while using ethanol, chloroform and aqueous extracts individually. Values are expressed in the mean \pm S.D. LC-W: *Litchi chinensis* water; LC-C: *Litchi chinensis* chloroform; LC-E: *Litchi chinensis* ethanol; GT-W: green tea water; GT-C: green tea chloroform; GT-E: green tea ethanol; O-W: olive water; O-C: olive chloroform; O-E: olive ethanol

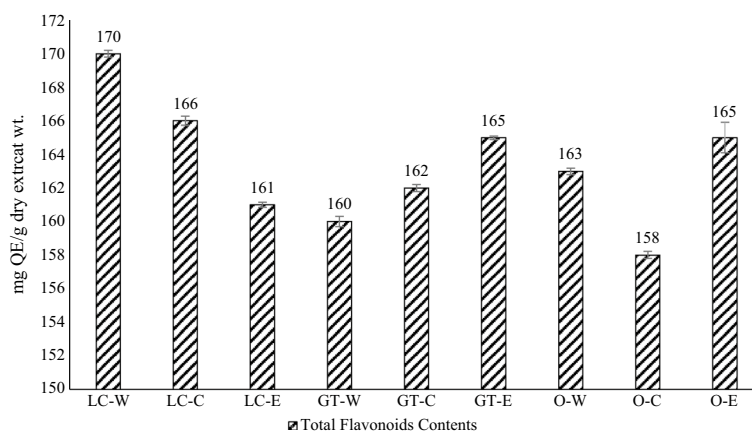


Fig. 2 Total flavonoid content (TFC) of leaf aqueous extracts, ethanol extracts, chloroform extract, and Aq: aqueous extracts. Values are expressed as the mean of three \pm S.D

Table 2 DPPH free radical scavenging activity of leave extracts

Sr. No.	Extract	Percentage scavenging			
		1000 $\mu\text{g/ml}$	750 $\mu\text{g/ml}$	500 $\mu\text{g/ml}$	IC50 $\mu\text{g/ml}$
1	Green tea (Aq)	83.0 \pm 2.6*	61.3 \pm 0.9*	23.3 \pm 0.8*	1050.8 \pm 5.4*
2	Green tea (EtOH)	74.4 \pm 0.6*	51.6 \pm 1.0*	17.7 \pm 0.6*	744.6 \pm 3.9*
3	Green tea (CHCl ₃)	76.4 \pm 0.9*	53.2 \pm 0.4*	17.6 \pm 1.2*	871.0 \pm 7*
4	Olive (Aq)	87.4 \pm 2.3*	64.4 \pm 0.6*	21.8 \pm 0.3*	931 \pm 6.1*
5	Olive (EtOH)	77.7 \pm 2.9*	52.2 \pm 1.2*	17.4 \pm 1.9*	734.2 \pm 3.2*
6	Olive (CHCl ₃)	82.2 \pm 0.3*	56.8 \pm 0.3*	16.5 \pm 0.6*	825.0 \pm 2.9*
7	Litchi C. (Aq)	85.6 \pm 3.4*	64.8 \pm 0.6*	33.4 \pm 1.0*	1228 \pm 5.7*
8	Litchi C. (EtOH)	89.5 \pm 1.6*	71.0 \pm 2.0*	35.8 \pm 0.5*	1298.6 \pm 5*
9	Litchi C. (CHCl ₃)	78.7 \pm 1.6*	51.0 \pm 2.5*	7.5 \pm 0.7*	739* \pm 2.2*
10	Ascorbic acid	98.5 \pm 3.3*	94.1 \pm 2.5*	91.3 \pm 2.8*	7.2*

Values were calculated as the mean of three \pm S.D

EtOH: ethanolic extract; Aq: aqueous extract; CHCl₃: chloroform extract

* $p < 0.05$ was considered statistically significant

Determination of antioxidant activity

Significant DPPH radical scavenger activity of aqueous leaf extracts, ethanol, and chloroform extracts was examined. The IC₅₀ value was determined by Graph-pad Prism software. As a positive control, ascorbic acid was used and observed IC₅₀ of 7.2 $\mu\text{g/ml}$ for DPPH radical. (Table 2). The IC₅₀ value of green tea was calculated as 1050 $\mu\text{g/ml}$, 744.6 $\mu\text{g/ml}$ and 871.0 $\mu\text{g/ml}$ for aqueous, ethanol and chloroform solvents, respectively. For olive leaf extracts the maximum percentage inhibition of 931.0 $\mu\text{g/ml}$, 734.2 $\mu\text{g/ml}$ and 825.0 $\mu\text{g/ml}$ was noted by using aqueous, ethanol and chloroform extracts, respectively. The IC₅₀ value of 1228 $\mu\text{g/ml}$, 1298.6 $\mu\text{g/ml}$ and 739 $\mu\text{g/ml}$ were noted, respectively.

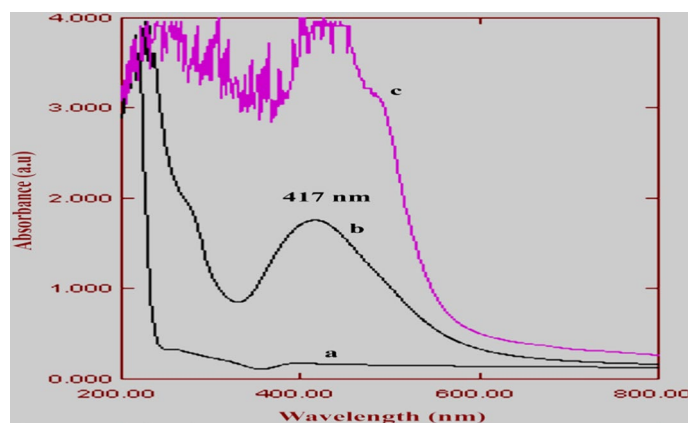


Fig. 3 UV-Vis spectrum of AgNP. **a** Silver nitrate solution, **b** biosynthesized silver nanoparticles; **c** *Litchi chinensis* leaf extract

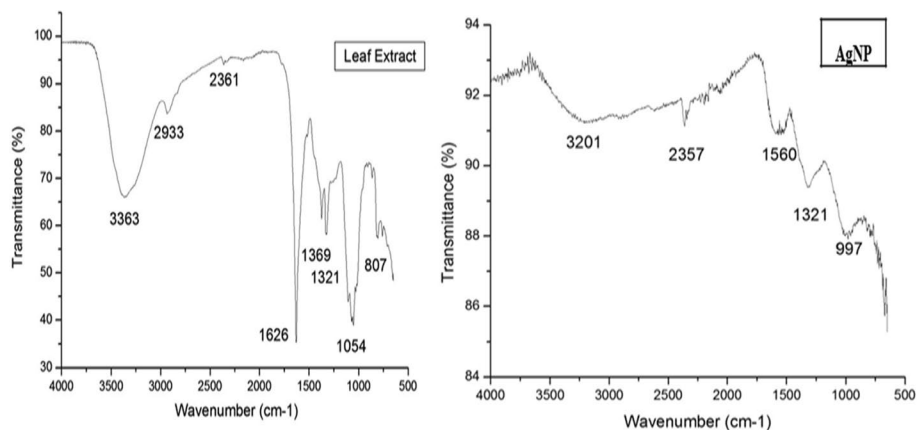


Fig. 4 FTIR spectra of leaf extract of *L. chinensis* and silver nanoparticles

Characterization of biosynthesized silver nanoparticles

The green synthesized silver nanoparticles were characterized by different methods, including UV-Vis spectroscopy, X-ray diffraction method, Fourier transform infrared spectroscopy, Energy dispersive spectroscopy, nano-size analyzer, and scanning electron microscopy.

UV-Vis spectroscopy

In the present study, 1 mM silver nitrate, green synthesized AgNP, and *Litchi chinensis* leaf extract were analyzed by UV-visible spectrophotometer in the range of 200–800 nm (Fig. 3). Aqueous AgNO₃ solution was observed without any characteristic peak. However, in the case of *Litchi chinensis* leaf extract, few peaks were observed due to the presence of phytochemicals. The silver nanoparticle showed maximum absorption (λ_{\max}) at 417 nm. This was a characteristic peak for the confirmation and initial characterization of silver nanoparticles (Iqbal et al. 2018).

Fourier transform infrared analysis (FTIR)

Biosynthesized AgNPs and *Litchi chinensis* extract were subjected to FTIR analysis for a comparative study of functional groups of both samples (Fig. 4). The absorption bands of leaf extract at 3363 cm^{-1} , 2933 and 2361 cm^{-1} , 1626 and 1321 cm^{-1} , 1054 cm^{-1} and 1369 cm^{-1} were caused by stretching vibration of O–H group, C–H-related groups, C=O group, C–O group, and bending of –CH bond into –CH₂, respectively. Below 1000 cm^{-1} , the absorption band at 807 cm^{-1} indicates the presence of the aliphatic C–H group. FTIR analysis of the biosynthesized AgNPs demonstrates the absorption bands at 3201 cm^{-1} , 2357 cm^{-1} , 1560 cm^{-1} , and 1321 cm^{-1} which were caused by stretching vibration of O–H group, stretching of alkyne bond in C=N group, involvement of secondary amines in the reduction process, and the presence of di-alkyl or aryl sulfone, respectively. Below 1000 cm^{-1} , the absorption band at 997 cm^{-1} was caused by aromatic alkenes.

X-ray diffraction analysis

X-ray diffraction analysis was performed to identify the crystalline nature of silver nanoparticles by obtaining characteristic peaks at 38.20° , 44.02° , 64.29° , and 77.22° that were attributed to 111, 200, 220, and 311 planes of nano-crystalline silver, respectively (Fig. 5). Two small peaks observed at 32° and 46° (star shape) were due to the presence of Ag₂O as an impurity, while other small peaks indicated the noise. The same result of XRD has been already published in our preliminary research (Iqbal et al. 2018).

Energy dispersive spectroscopy (EDS)

The presence of metallic silver particles was determined by energy dispersive spectroscopy. The absorption band for silver metallic atoms was recorded at a 2.984 keV band position. The atomic percentage of silver was noted as 0.76%, with 25.61 counts. The counts for silver metallic atoms were low, since drops of AgNPs were coated on silicon wafers for SEM and EDS. On the other hand, a strong peak of silicon was observed at the 1.739 keV band position due to the preparation of the sample on silicon wafers (Fig. 6).

Scanning electron microscopy (SEM)

SEM analysis was used to determine the shape and size of AgNPs by placing a drop of AgNP solution on a silicon wafer in SEM. Well dispersed spherical NPs with a diameter

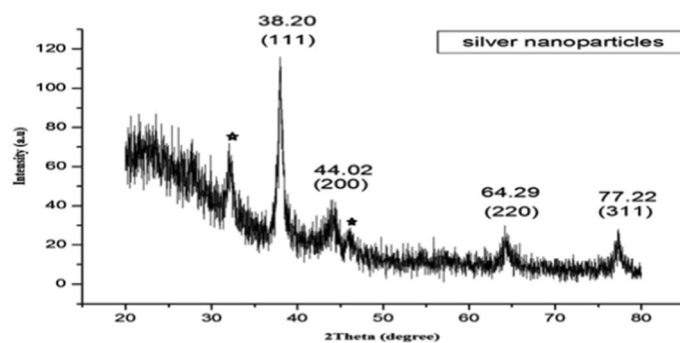


Fig. 5 X-ray diffraction pattern of biosynthesized silver nanoparticles

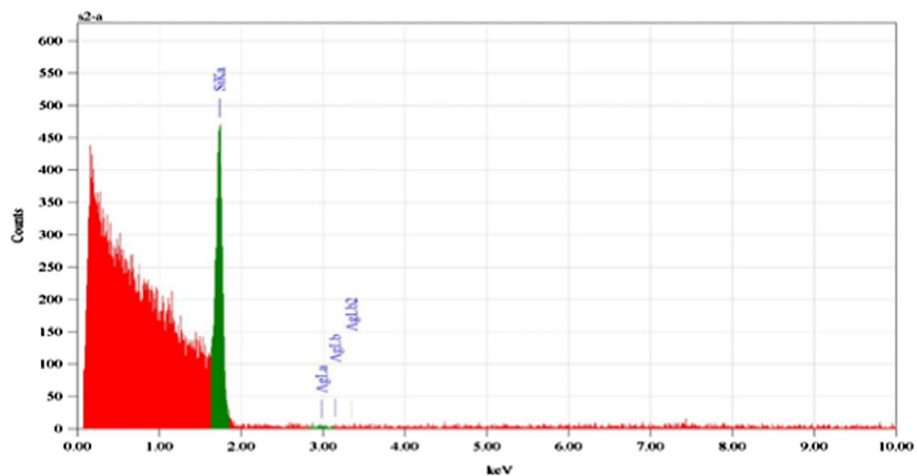


Fig. 6 Energy dispersive spectroscopy of biosynthesized silver nanoparticles

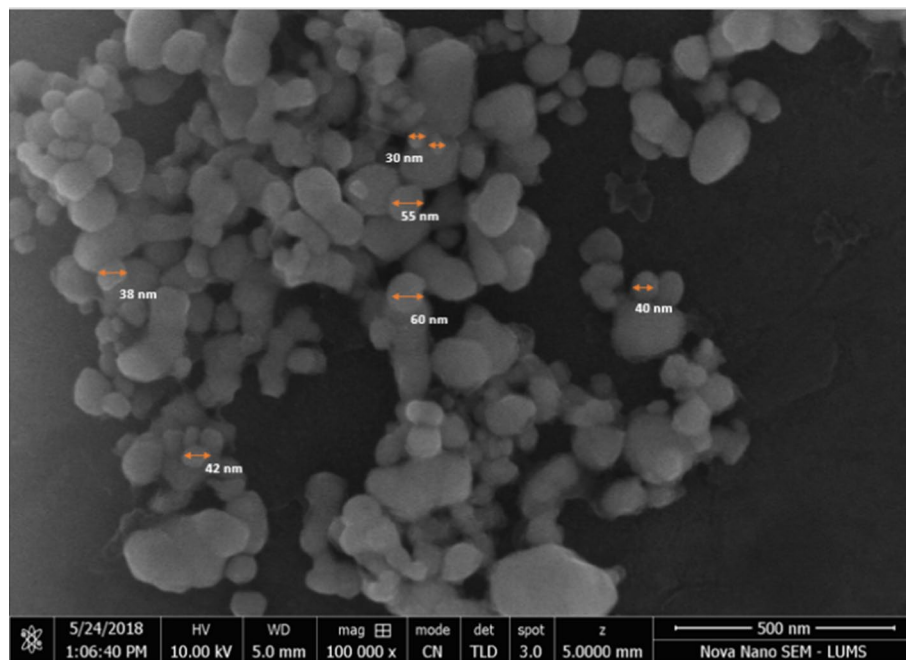


Fig. 7 Scanning electron microscope image of biosynthesized silver nanoparticles

range of 41–55 nm were observed (Fig. 7). Larger sized nanoparticles were the result of the aggregation of smaller ones.

Cellular transfection of microRNA34a mimics and silver nanoparticles

MCF-7 cell line was selected to investigate the treatment response and to evaluate the anticancer potential by using three different treatment strategies. (i) Micro RNA34a mimics (miR34a), (ii) silver nanoparticles, (iii) co-delivery of miR34a mimics with silver nanoparticles. Transfection was successfully achieved by using OPTI-MEM media and Lipofectamine 3000 as a transfecting reagent. All the experimental procedures were performed in duplicate (Additional file 1).

RNA isolation, cDNA synthesis, and mRNA expression analysis of targeted genes by qRT-PCR

After successful transfection of miR34a mimics and AgNPs in the human MCF7 breast cancer cell line, RNA was extracted and subjected to quantitative real-time PCR for comparative expression analysis by taking GAPDH as a housekeeping gene, and to evaluate the expression of “DR4 and DR5” genes that play a crucial role in the onset of apoptosis.

For the comparative gene expression analysis, housekeeping genes Glyceraldehyde-3-phosphate dehydrogenase “GAPDH” was used. Expression levels of GAPDH mRNA were measured by using qRT-PCR with specific target genes DR4 and DR5.

Amplification of targeted genes DR4 (TNFRSF10A) and DR5 (TNFRSF10B) was performed by qRT-PCR (Additional file 1). Results indicate that the expression of DR4 was up-regulated by 0.8-fold and 0.5-fold after treatment with green-derived silver nanoparticles and miR34a mimics, respectively. Likewise, the expression of DR5 was also up-regulated by 3.7-folds and 1.0-folds after treatment with green-derived silver nanoparticles and miR34a mimics, respectively. Whereas, co-delivery of miR34a mimics and silver nanoparticles together down-regulate the expression of DR4 and DR5 by 0.3-folds.

Comparative qPCR expression analysis of DR4 and DR5

Comparative analysis of DR4 and DR5 genes was performed by taking GAPDH as an internal control. After three different treatments, it was concluded that green-derived silver nanoparticles from *Litchi chinensis* leaf extract are more efficient against cancer, particularly in the case of DR5 when compared with DR4 by using silver nanoparticles individually. However, when compared with the co-delivery of silver nanoparticles with miR34a mimics, a decreased expression was observed (Fig. 8).

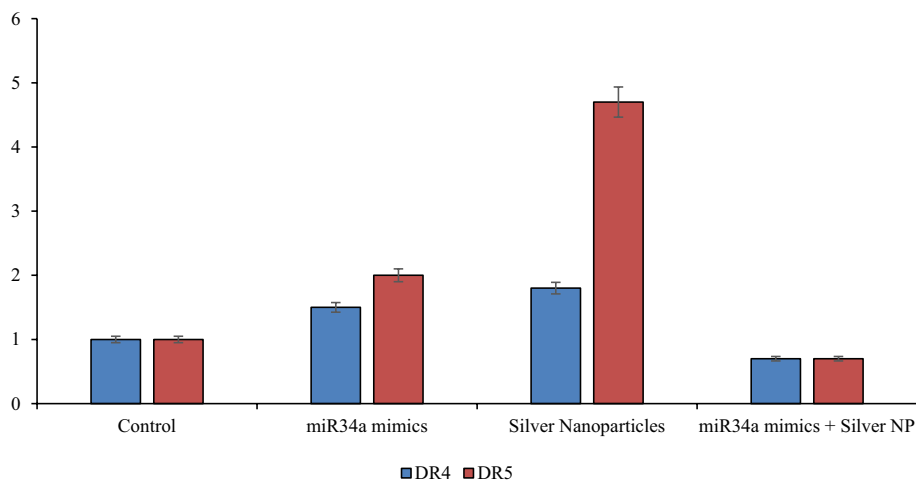


Fig. 8 Comparative expression analysis of DR4 and DR5 by taking GAPDH as an internal control. Silver nanoparticles alone show higher expression than the other two treatments

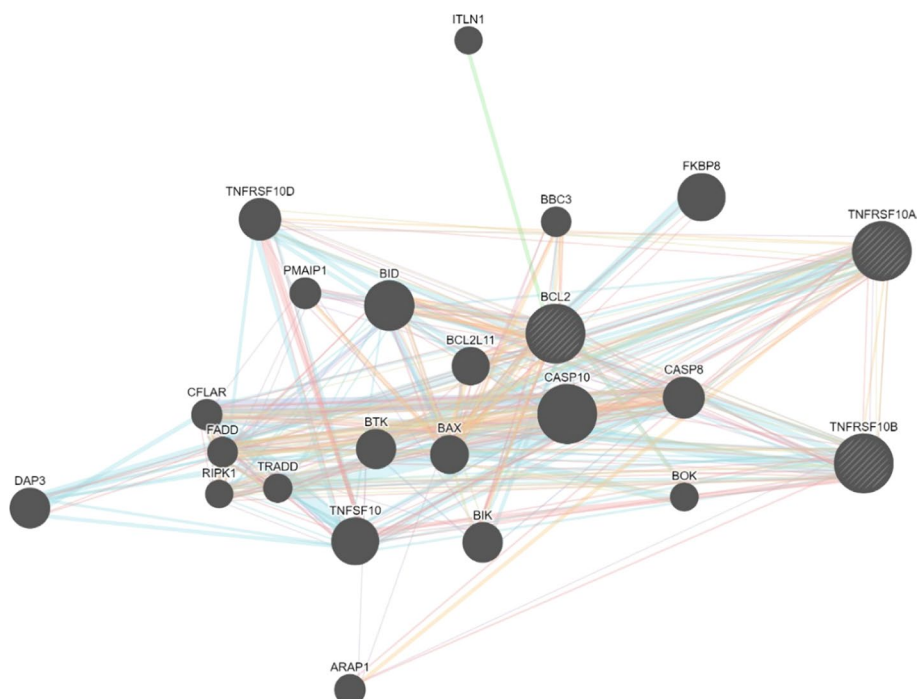


Fig. 9 DR4 (TNFRSF10A) and DR5 (TNFRSF10B) signaling pathways to induce apoptosis

DR4 and DR5 signaling interaction with Casp8 and Casp10 to induce apoptosis

Bioinformatic tool (Genemania) was used to establish a supporting link that DR5 (TNFRSF10B) has significant interaction with Caspase 8 and Caspase 10. These caspases cascade plays a decisive role in apoptotic stimulation by targeting the Bcl-2 protein (Fig. 9). These findings also highlighted the important role of DR5 to induce cellular apoptosis by using silver nanoparticles. Silver nanoparticles are also reported to directly interact with p53 and negatively regulate Bcl-2 (Gurunathan et al. 2015).

Conclusions

Cancer heterogeneity and multiple drug resistance behaviors make it difficult to limit the abnormal growth of cancer cells. To improve the therapeutic effect against cancer growth, nanotechnology-based pharmaceutical strategies could be a significant tool. In this study, nanoparticles were synthesized using *Litchi chinensis* leaf extracts. *Litchi chinensis* leaf extracts are reported to have an optimum antioxidant potential, and sufficient phenolic and flavonoid contents. In addition to nanoparticles, miR34a mimics were also incorporated to determine their anti-cancer by evaluating the expression of targeted genes. Successful cellular transfection was achieved by using lipofectamine 2000 in MCF-7 cell lines.

It has been shown that apoptosis is directly associated with DR4 and DR5 pathways. The expression of both genes was investigated after successful delivery of silver nanoparticles, miR34a mimics, and co-delivery of silver nanoparticles and miR34a together. It was observed that transfection of silver nanoparticles upregulated the expression of DR4 and DR5 by 0.8- and 3.7-folds, respectively. miR34a was noted to upregulate the

expression of DR4 and DR5 by 0.5- and 1.0-folds, respectively. Surprisingly, the co-delivery of miR34a mimics and silver nanoparticles reduced the expression level of both genes. It can be concluded that the co-delivery of silver nanoparticles and miR34a mimics compete with the promotor binding region of all the targeted genes. But still, more research investigations regarding molecular mechanisms in the future involving humanized mice models are required to determine active compounds in *Litchi chinensis* and use a nano-coating approach to target the molecular sites specifically.

Supplementary Information

The online version contains supplementary material available at <https://doi.org/10.1186/s12645-022-00137-8>.

Additional file 1. Fold expression of DR4 and DR5 genes.

Acknowledgements

We thank Dr. Muhammad Ismail, Ammad Ahmed Farooqi (IBGE, KRL Lab, Islamabad), and Dr. Murtaza Saleem (LUMS, Lahore) for their extensive support and help to provide facilities to use cell lines and for the characterization of nanoparticles.

Author contributions

Conceptualization and design were performed by MJJ, UR, ZJ, JS-R, MB, WCC; validation, investigation, methods, experimental assays, data curation, and writing were performed by MJJ, ZH, KI, AK, SR, ZMA, I-CB, RVB, IS, AY, SDD; review and editing were performed by UR, ZJ, ŽR, JS-R, MB and WCC. All authors read and approved the final manuscript.

Funding

Not applicable.

Availability of data and materials

Not applicable.

Declarations

Ethics approval and consent to participate

Not applicable.

Consent for publication

Not applicable.

Competing interests

Authors wish to confirm that there are no known conflicts of interest associated with this publication and there has been no significant financial support for this work that could have influenced its outcome.

Author details

¹Department of Biochemistry and Biotechnology, University of Gujrat, Gujrat, Pakistan. ²Department of Biotechnology, University of Sialkot, Sialkot, Pakistan. ³Office of Research Innovation and Commercialization, Lahore Garrison University, Lahore, Pakistan. ⁴Department of Chemistry, College of Science, King Saud University, P. O. Box 2455, Riyadh 11451, Saudi Arabia. ⁵University Hospital Centre Zagreb, Zagreb, Croatia. ⁶Department of Microbiology, Victor Babes University of Medicine and Pharmacy of Timisoara, Timisoara, Romania. ⁷Multidisciplinary Research Center on Antimicrobial Resistance, Timisoara, Romania. ⁸Preventive Medicine Study Center, Victor Babes University of Medicine and Pharmacy of Timisoara Department of Microbiology, Timisoara, Romania. ⁹University of Life Sciences "King Mihai I" from Timisoara, 300645, Calea Aradului 119, Timis, Romania. ¹⁰Facultad de Medicina, Universidad del Azuay, Cuenca, Ecuador. ¹¹Biomedical Research Centre, Al-Farabi Kazakh National University, Al-Farabi Av. 71, 050040 Almaty, Kazakhstan. ¹²Department of Biology, Faculty of Science, Sivas Cumhuriyet University, 58140 Sivas, Turkey. ¹³Beekeeping Development Application and Research Center, Sivas Cumhuriyet University, 58140 Sivas, Turkey. ¹⁴Department of Clinical Oncology, Queen Elizabeth Hospital, Kowloon, Hong Kong.

Received: 4 May 2022 Accepted: 26 September 2022

Published online: 11 October 2022

References

- Abdelhady NM, Badr KA (2016) Comparative study of phenolic content, antioxidant potentials and cytotoxic activity of the crude and green synthesized silver nanoparticles' extracts of two Phlomis species growing in Egypt. *J Pharmacogn Phytochem* 5(6):377–383
- Ahmed S et al (2016) A review on plants extract mediated synthesis of silver nanoparticles for antimicrobial applications: a green expertise. *J Adv Res* 7(1):17–28

- Awwad AM, Salem NM (2012) Green synthesis of silver nanoparticles by mulberry leaves extract. *Nanosci Nanotechnol* 2(4):125–128
- Carvalho M et al (2010) Human cancer cell antiproliferative and antioxidant activities of *Juglans regia* L. *Food Chem Toxicol* 48(1):441–447
- Chatterjee T et al (2015) Antibacterial effect of silver nanoparticles and the modeling of bacterial growth kinetics using a modified Gompertz model. *Biochim Biophys Acta (BBA) Gen Subj* 1850(2):299–306
- Fu L et al (2011) Antioxidant capacities and total phenolic contents of 62 fruits. *Food Chem* 129(2):345–350
- Gaur U, Aggarwal BB (2003) Regulation of proliferation, survival and apoptosis by members of the TNF superfamily. *Biochem Pharmacol* 66(8):1403–1408
- Gurunathan S et al (2015) Comparative assessment of the apoptotic potential of silver nanoparticles synthesized by *Bacillus tequilensis* and *Calocybe indica* in MDA-MB-231 human breast cancer cells: targeting p53 for anticancer therapy. *Int J Nanomed* 10:4203
- Han H et al (2017a) Hypertension and breast cancer risk: a systematic review and meta-analysis. *Sci Rep* 7(1):1–9
- Han H et al (2017b) Hypertension and breast cancer risk: a systematic review and meta-analysis. *Sci Rep* 7:44877
- He R et al (2002) Preparation of polychrome silver nanoparticles in different solvents. *J Mater Chem* 12(12):3783–3786
- Imani S et al (2017) The diagnostic role of microRNA-34a in breast cancer: a systematic review and meta-analysis. *Oncotarget* 8(14):23177
- Iqbal MJ et al (2018) Biosynthesis of silver nanoparticles from leaf extract of *Litchi chinensis* and its dynamic biological impact on microbial cells and human cancer cell lines. *Cell Mol Biol* 64(13):42–47
- Khalil MM et al (2014) Green synthesis of silver nanoparticles using olive leaf extract and its antibacterial activity. *Arab J Chem* 7(6):1131–1139
- Kiraz Y et al (2016) Major apoptotic mechanisms and genes involved in apoptosis. *Tumor Biol* 37(7):8471–8486
- Livak KJ, Schmittgen TD (2001) Analysis of relative gene expression data using real-time quantitative PCR and the $2^{-\Delta\Delta CT}$ method. *Methods* 25(4):402–408
- Pathak Y, Thassu D (2016) Drug delivery nanoparticles formulation and characterization, vol 191. CRC Press, Boca Raton

Publisher's Note

Springer Nature remains neutral with regard to jurisdictional claims in published maps and institutional affiliations.

Ready to submit your research? Choose BMC and benefit from:

- fast, convenient online submission
- thorough peer review by experienced researchers in your field
- rapid publication on acceptance
- support for research data, including large and complex data types
- gold Open Access which fosters wider collaboration and increased citations
- maximum visibility for your research: over 100M website views per year

At BMC, research is always in progress.

Learn more biomedcentral.com/submissions

